Effects of Water on the Structure and Bonding of Resorcinol in the Interlayer of Montmorillonite Nanocomposite: A Periodic First Principle Study

Abhijit Chatterjee,*,†,‡ Takeo Ebina,‡ and Fujio Mizukami‡

Accelrys K.K., Nishishinbashi TS Building 11F, 3-3-1 Nishishinbashi, Minato-ku, Tokyo 105-0003, Japan, and Laboratory of Membrane Chemistry, National Institute of Advanced Industrial Science and Technology, AIST Tohoku, 4-2-1 Nigatake, Miyagino-ku, Sendai 983-8551, Japan

Received: September 17, 2004; In Final Form: February 14, 2005

Resorcinol forms a novel nanocomposite in the interlayer of montmorillonite. This resorcinol oligomer is stable inside the clay matrixes even above the boiling point of the monomer. A periodic ab initio calculation was performed with hydrated and nonhydrated montmorillonite before and after intercalation of resorcinol. For the most feasible dimer and tetramer shaped oligomer of resorcinol, the intramolecular and intermolecular hydrogen bonding feasibility has been tested using the DFT-BLYP approach and the DNP basis set in the gas phase and in the presence of aqueous solvent. After locating the active site through Fukui functions within the helm of the hard−soft acid−base principle, the relative nucleophilicity of the active cation sites in their hydrated state has been calculated. A novel quantitative scale in terms of the relative nucleophilicity and electrophilicity of the interacting resorcinol oligomers before and after solvation is proposed. Besides that, a comparison with a hydration situation and also the strength of the hydrogen bridges have been evaluated using mainly the dimer and cyclic tetramer type oligomers of resorcinol. Using periodic ab initio calculations, the formation mechanism was traced by the following two ways: (1) resorcinol molecules combine without any interaction with water or (2) resorcinol oligomerizes through water. Both the mechanism is compared and the effect of water on the process is elucidated. The results show that resorcinol molecules combine after hydration only and hence they are stable at higher temperature. The fittings of the oligomers were also tested as well by periodic calculation to compare the stability of the oligomers inside the newly formed clay nanocomposite.

Introduction

Clays are lamellar aluminosilicates with a large variety of physicochemical properties such as swelling, adsorption, surface acidity, ion exchange, etc. Smectite, a member of the 2:1 dioctahedral structural unit layer, has three sheets; one octahedral sheet is sandwiched between two tetrahedral sheets. This octahedral sheet consists of two sheets of closely packed oxygen and hydroxyls in which aluminum, iron, or magnesium atoms are embedded in octahedral coordination, so that they are equidistant from six oxygen atoms or hydroxyls. On the other hand, the tetrahedral silicon atom in each tetrahedron is equidistant from four oxygen atoms or hydroxyls. The silica tetrahedral groups are arranged to form a hexagonal network, which is repeated indefinitely to form a sheet of composition $Si_4O_6(OH)_4$. Montmorillonite is a member of the 2:1 dioctahedral smectite family in which the two tetrahedral sites sandwich a sheet of octahedrally coordinated metal ions. Substitution of a bivalent metal ion for octahedral aluminum in montmorillonite results in a net negative layer charge and the interaction with positive ions (exchangeable cation) to form an interlayer hydrated phase. There also exists a high repulsive potential on the surface resulting from isomorphous substitution.

Synthesis of intercalated clay material with well-defined compositions and basal spacing was described previously.[1] Organic ammonium ions and neutral organic molecules are intercalated in the interlayer space between the silicate layers. Recent studies in this area show that polymers can be successfully encapsulated between smectite clay layers of about 1 nm thickness.[2−5] Many experimental studies have reported the syntheses of polystyrene,[6,7] poly(acrylic acid),[8] and polyacrylonitrile[9] inside the clay layer. Pinnavaia et al.[10] had intercalated a polyamic acid in the galleries of a series of $CH_3-(CH_2)_{n-1}NH_3^+$ montmorillonite. This resulted in the conversion of polyamic acid to polyimide. This polymer nanocomposite improves the barrier film properties of the polymer. It is observed that the polymer-hybrid of clay is often superior to the conventional composite material. Compared to conventional polymer microcomposites, polymer−clay nanocomposites possess improved mechanical, thermal, and barrier properties for as low as 2% (weight) of clay content.[11] Usuki et al.[12] have successfully described the manyfold increase of tensile strength and thermal and rheological properties through the incorporation of montmorillonite clay to nylon. As observed from some earlier work,[13,14] the platelike structure of the clay particles embedded in a polymer matrix generally reduces the gas permeability. There are very few theoretical studies on the structure−property relationship of nanocomposites. Recently, Gardebien et al.[15] performed a molecular dynamics (MD) study on the poly(ϵ-caprolactum)−montmorillonite clay nanocomposite, to propose the structure and energetics of the chains intercalated inside the

* To whom correspondence should be addressed. E-mail: c-abhijit@aist.go.jp or achatterjee@accelrys.com. Phone: +81-03-3578-3861. Fax: +81-03-3578-3873.

† Accelrys K.K.

‡ Laboratory of Membrane Chemistry, National Institute of Advanced Industrial Science and Technology, AIST Tohoku.

10.1021/jp045775z CCC: $30.25
Published on Web 03/19/2005

clay matrix. Manias and co-workers have studied the polymer/nanocomposite both by experiment and by MD simulation.[16,17]

We have synthesized clay nanocomposites with resorcinol.[18] Self-supported nanocomposite films are prepared by the casting method, and the films mostly consist of phyllosilicate. A small amount of organic material is added to strengthen the film. The resultant films are translucent, flexible, and highly stable.

In our earlier study,[19−22] we rationalized the structure−property relationship in montmorillonite clays and observed that the hydroxyl groups present in the clay structure play a crucial role in the catalytic activity. We have explored the role of layer charge on the catalytic activity of two different types of smectite clay in the presence of common exchangeable cation sodium with a single water molecule.[23] It is observed that interlayer cation (Na^+) has a lesser influence on hydrogen bond formation in the presence of a single water molecule. This encourages us to study the hydrated cations at least at their first layer of hydration. Previously, we have used[24] both localized and periodic calculations on a series of monovalent (Li^+, Na^+, K^+, Rb^+, Cs^+) and divalent (Mg^{2+}, Ca^{2+}, Sr^{2+}, Ba^{2+}) cations to monitor their effect on the swelling of clays. The activity order obtained for the exchangeable cations among all the monovalent and divalent series studied is $Ca^{2+} > Sr^{2+} > Mg^{2+} > Rb^+ > Ba^{2+} > Na^+ > Li^+ > Cs^+ > K^+$.

The hard−soft acid−base (HSAB) principles classify the interaction between acids and bases in terms of global softness. Pearson proposed the global HSAB principle.[25] The global hardness was the second derivative of energy with respect to the number of electrons at constant temperature and external potential, which includes the nuclear field. The global softness is the inverse of this. Pearson also suggested a principle of maximum hardness (PMH),[26] which stated that, for a constant external potential, the system with the maximum global hardness is most stable.

In recent days, density functional theory (DFT) has gained widespread use in quantum chemistry. Some DFT-based local properties, like Fukui functions and local softness,[27] have already been used for reliable predictions in various types of electrophilic and nucleophilic reactions in the case of zeolites and clay materials.[28−31] Generally, compared to a gas-phase calculation, the solvent environment alters the charge distribution of a molecule. There is an increase in the dipole moment of molecules such as water which enhances the intrinsic reactivity of polar molecules toward nucleophilic and electrophilic attack.[32]

Our aim in the current work is to rationalize the formation process of the resorcinol clay nanocomposite in the context of clay solvation. Keeping in mind the swelling property of clay, we wish to explore the role of water in the structure and bonding of resorcinol in the interlayer of the montmorillonite type of clay. We have used DFT-based local descriptors for calculating the reactivity index within the helm of the HSAB principle. It is used to determine the possible correlation between clay and the resorcinol matrix. Finally, we have performed the periodic calculation to foresee the fitting of the resorcinol oligomer inside the interlayer of clay, to develop an idea about the probable size of the oligomer inside the clay interlayer.

Theory

In density functional theory, hardness (η) is defined as[33]

$$\eta = (1/2)(\delta^2 E/\delta N^2)v(r) = (1/2)(\delta\mu/dN)_v$$

where E is the total energy, N is the number of electrons of the chemical species, and μ is the chemical potential.

The global softness, S, is defined as the inverse of the global hardness, η.

$$S = 1/2\eta = (\delta N/\delta\mu)_v$$

Using the finite difference approximation, S can be approximated as

$$S = 1/(\mathrm{IE} - \mathrm{EA}) \quad (1)$$

where IE and EA are the first ionization energy and electron affinity of the molecule, respectively.

The Fukui function $f(r)$ is defined by[27]

$$f(r) = [\delta\mu/dv(r)]_N = [\delta\rho(r)/\delta N]_v \quad (2)$$

The function f is thus a local quantity, which has different values at different points in the species, N is the total number of electrons, μ is the chemical potential, and v is the potential acting on an electron due to all nuclei present. Since $\rho(r)$ as a function of N has slope discontinuities, eq 1 provides the following three reaction indices:[27]

$$f^-(r) = [\delta\rho(r)/\delta N]_v^- \quad \text{(governing electrophilic attack)}$$

$$f^+(r) = [\delta\rho(r)/\delta N]_v^+ \quad \text{(governing nucleophilic attack)}$$

$$f^0(r) = (1/2)[f^+(r) + f^-(r)] \quad \text{(for radial attack)}$$

In a finite difference approximation, the condensed Fukui function[34] of an atom, say x, in a molecule with N electrons is defined as

$$f_x^+ = [q_x(N+1) - q_x(N)] \quad \text{(for nucleophilic attack)} \quad (3)$$

$$f_x^- = [q_x(N) - q_x(N-1)] \quad \text{(for electrophilic attack)}$$

$$f_x^0 = [q_x(N+1) - q_x(N-1)]/2 \quad \text{(for radical attack)}$$

where q_x is the electronic population of atom x in a molecule.

The local softness $s(r)$ can be defined as

$$s(r) = (\delta\rho(r)/\delta\mu)_v \quad (4)$$

Equation 3 can also be written as

$$s(r) = [\delta\rho(r)/\delta N]_v[\delta N/\delta\mu]_v = f(r)S \quad (5)$$

Thus, local softness contains the same information as the Fukui function $f(r)$ plus additional information about the total molecular softness, which is related to the global reactivity with respect to a reaction partner, as stated in the HSAB principle. Atomic softness values can easily be calculated by using eq 4, namely,

$$s_x^+ = [q_x(N+1) - q_x(N)]S \quad (6)$$

$$s_x^- = [q_x(N) - q_x(N-1)]S$$

$$s_x^0 = S[q_x(N+1) - q_x(N-1)]/2$$

Computational Methodology and Model

The software package CASTEP (Cambridge Serial Total Energy Package), which has been described elsewhere,[35,36] and associated programs for symmetry analysis were used for the calculations. CASTEP is a pseudo-potential total energy code that employs Perdew and Zunger[37] parametrization of the

exchange-correlation energy, super cells and special point integration over the Brillouin zone and a plane wave basis set for the expansion of the wave functions. The methodology has been used in mineralogy to examine the hydration of corderite.[38] Becke−Perdew parametrization[39,40] of the exchange-correlation functional, which includes gradient correction (generalized gradient approximation, GGA), was employed, as this is a well-established technique.[41,42] The pseudo-potentials are constructed from the CASTEP database. The screening effects of core electrons are approximated by local density approximation (LDA), while the screening effects for valence electrons are approximated by GGA. This is a reasonable approximation as shown by Garcia et al.[43] To obtain equilibrium structures for a given set of lattice constants, ionic and electronic relaxations were performed using the adiabatic or "Born−Oppenheimer" approximation, where the electronic system is always in equilibrium with the ionic system. Relaxations were continued until the total energy had converged. In the present calculations, kinetic cutoff energies between 600 and 1500 eV have been used. The Monkhorst−Pack scheme[44] was used to sample the Brillouin zone. The calculations were restricted to one special K point in the Brillouin zone, placed at (0.0, 0.0, 0.0).

In the present study, all calculations have been carried out with DFT[45] using the DMOL^3 code of Accelrys Inc. A gradient corrected functional BLYP[46,47]and DNP basis set[48] was used throughout the calculation. Basis set superposition error (BSSE) was also calculated for the current basis set in nonlocal density approximation (NLDA) using the Boys−Bernardi method.[49] Single point calculations of the cation and anion of each molecule at the optimized geometry of the neutral molecule were also carried out to evaluate Fukui functions, global and local softness. The condensed Fukui function and atomic softness were evaluated using eqs 3 and 6, respectively. The gross atomic charges were evaluated using the technique of electrostatic potential (ESP) driven charges.

The ideal formula of the clay montmorillonite is $(M^+_x, nH_2O)(Al_{4-x}Mg_x)Si_8O_{20}(OH)_4$,[21] where $x = (12 - a - b)$ is the layer charge, and M is the balancing cation either monovalent or divalent. The desired structure of montmorillonite with the formula $MSi_8Al_3MgO_{20}(OH)_4$ has been generated from the structure of well-defined pyrophillite.[50] Hydrated phases were calculated using the procedure mentioned elsewhere.[24] The calculations were performed with the minimum energy structures of the clays at the unhydrated phase. The interlayer structure was held fixed and the interlayer spacing was manipulated to accommodate the resorcinol oligomer; both the dimer and tetramer form were calculated. For the calculation with the resorcinol oligomer, we relaxed the cation, water, resorcinol oligomer, and the interlayer space. The lower part of the structure was kept fixed to compromise between CPU cost and accuracy.

Results and Discussion

We have performed ab initio pseudo-potential calculations on a nanocomposite of resorcinol intercalated montmorillonite, to understand the structure of the intercalated compound and to propose a plausible mechanism of the oligomerization process of resorcinol. We have monitored the interaction of water with resorcinol in the presence of clay moiety to understand the role of water whether in swelling or the oligomerization process of resorcinol. In the swelling phenomena of clay, it is generally observed that the interlayer cation has a lesser influence on hydrogen bond formation in the presence of a single water molecule. Moreover, from our recent study[24] we found that for a single hydration layer, swelling of the clay structure occurs in the *c* direction after hydration. So far, different theoretical and experimental groups observed that the interlayer water orientation depends mainly on cation location; if the cation lies closer to the clay layers the influence on interlayer water is weak, whereas the degree of hydrogen bonding among water molecules is greater as the cation stays away from the clay layer. In clay swelling, there exist two kinds of water molecule, one bonded to the interlayer cation in its hydration shell and another, the nonbonded water, lying as a bulk. In the presence of the hydration shell, the activity of the compensating cation is zero in the bulk water and positive in the clay suspension. The cations must move from the clay suspension to the bulk water to equalize their activity. The solvation interaction is a short-range interaction; therefore, to rationalize the swelling phenomenon one needs to concentrate on only the water molecules present in the hydration shell. There is a consensus in the fact that clay swelling is dependent on humidity. An increase in humidity will increase the hydration layer, and after reaching three layers of hydration it will saturate. Any further addition of water does not modify either the hydration shells of the clay surface or the interlamellar cations. Here, as we are considering the water interaction with resorcinol, we first looked at the resorcinol monomer and its possible oligomers in the gas phase and in the solvent phase. First we optimized the geometry of the oligomer both unsolvated and in solvent medium, followed by the periodic calculation of the resorcinol oligomer in the presence of water and cation to determine the fitting of the oligomer inside the clay interlayer.

Activity of Clay Cluster and Resorcinol Molecules in Terms of Reactivity Index. In our earlier study,[24] we have observed that the hydroxyl hydrogen present in montmorillonite (where Mg^{2+} replaces one of the Al^{3+} ions present at the octahedral site) is more active than the beidellite type (where tetrahedral Si^{4+} is replaced by Al^{3+}) of clays whereas the reverse is true for structural hydroxyl groups. Moreover, in terms of localized reactivity index, the hydroxyl hydrogens of 2:1 smectite clays can behave as a nucleophilic center, which can then interacts with an electrophilic site.

In the experimental procedure, the resorcinol molecule is mixed with the hydrated montmorillonite clay moiety before a heat treatment condition is applied. Using the reactivity index theory, we wish to compare the electrophilicity and nucleophilicity of the constituent atoms in the gas phase and solvated phase to unfold the role of solvation in the intramolecular configuration. We have calculated the common resorcinol oligomer configurations such as monomer, dimer, and tetramer both in the gas phase and in the solvated phase. The structures of the resorcinol molecules starting from monomer through dimer to tetramer in the gas phase and solution phase are shown in Figures 1−3. The results for the monomer are revealed in Table 1. All those constituent atoms are labeled as shown in Figure 1a,b. Considering hydroxyl group of atoms, results show that the solvated resorcinol monomer has higher global softness. For some cases, the Fukui functions and the softness values are very close. So it would be difficult to formulate a trend, to elucidate the possibility of short-range intermolecular H-bonding between the resorcinol and water molecules. Hence, it seems to be a distinguished idea to calculate the ratio of s_x^+ and s_x^-, termed as relative electrophilicity or nucleophilicity. To predict intramolecular and intermolecular reactivity sequences of carbonyl compounds, Roy et al.[51] first proposed the idea of relative nucleophilicity/electrophilicity, the ratio of electrophilicity and nucleophilicity of a particular atom center. We have used the

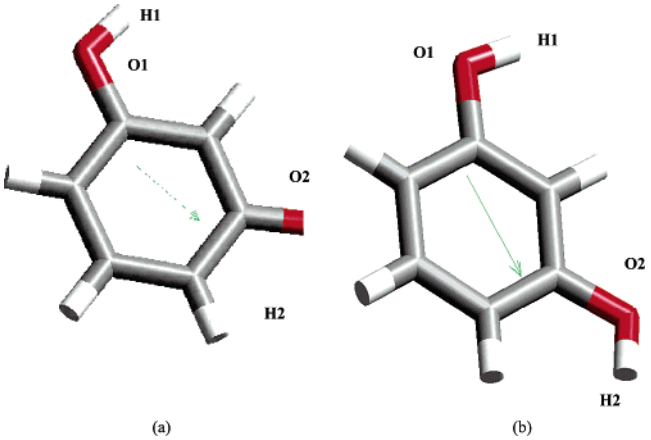

Figure 1. Optimized geometry of the resorcinol monomer in (a) the gas phase and (b) the solvated phase with all the hydrogen and oxygen atoms of the molecule labeled.

method for the first time to find the best dioctahedral smectite for nitrogen heterocyclic adsorption[52] and for the adsorption property of para- and meta-substituted nitrobenzene.[53] The results of relative nucleophilicity s_x^+/s_x^- and electrophilicity s_x^-/s_x^+ are shown in Tables 1−4. The reactivity index calculation for the monomer of resorcinol (Table 1) shows that H1 is more electrophilic and O2 is more nucelophilic among the constituent atoms. The trend is the same for both the gas phase and solvated phase. It is also observed from the relative electrophilicity and nucleophilicity that the relative nucleophilicity increases on solvation whereas the relative electrophilicity decreases on solvation. Figure 2a,b represents the gas phase and the solvated phase of the resorcinol dimer molecule, respectively. The O2 and H2 of the two monomers combine to form a new O3 in the resulting resorcinol dimer; hence the other hydroxyl group present with atomic nomenclature O1 and H1 remains unaffected. The results for the dimer are indicated in Table 2. The relative nucleophilicity/electrophilicity shows a similar trend as observed for the monomer, but the amount of increment or decrement after solvation is much more pronounced in the dimer. Here, understandably the most electrophilic moiety is H1 and the most nucleophilic moiety is the O3 center. During the formation of the tetramer, the O1 and H1 of the dimer combine to form a new O4 center. So the identity of the monomer O1 and O2 changes to O3 and O4 after formation of the tetramer. The atom centers were labeled in Figure 3a to represent the gas phase and in Figure 3b for the solvated phase. The results shown in Table 3 bring out an interesting phenomenon. We now find that O3 is more nucleophilic than O4 present in the tetramer. It is as well observed that the relative electrophilicity now increases after solvation and the relative nucleophilicity decreases after solvation. The trend is just the opposite for monomer and dimer and suggested that the dimer will favor more intramolecular interaction compared to that of the tetramer. Dimers with higher nucleophilicity will be favorably interacting with sites of increasing electrophilicity and proceed toward the intramolecular bonding. According to the intermolecular interaction concept,[53] the pseudo-bond formation exists between two centers with matching electrophilicity and nucleophilicity. Generally, for the clay the hydroxyl hydrogen acts as a nucleophilic center. If two nucleophilic sites come together and interact after solvation, they cannot be stable inside the clay. But experimental facts suggested that the material is stable enough, though we do not know which form of resorcinol is inside. Hence, this diversion between theory and experimental fact indicates that there must be some other parameters, which dominate the procedure. The ambiguity here is that we have so far only looked at the resorcinol molecule in the solvated form but in reality, there exist clay, interlayer cation, water, and resorcinol. So the first step in the process is hydration of the resorcinol molecule. As we observed before,[24] at a highest humidity of 90% three hydration layers around the cation exist. Therefore, the molecule incorporated in the interlayer of clay will have equal probability to be hydrated rather than solvated with the rest of the bulk water molecule. Similarly, some chance of partial hydration of the molecule cannot be ignored. This will propose the preference of the resorcinol active centers to interact with water, which further postulates the mechanism of the interaction between resorcinol and water molecule. The gas-phase structure along with the hydrated structure of the resorcinol monomer is shown in Figure 4a,b, respectively. The results in Table 4 suggested an unusual phenomenon. In terms of localized reactivity index, the same atomic center of the resorcinol molecule produces the maximum electrophilicity and nucleophilicity. The electrophilicity is increasing after hydration and favors the interaction with the clay lattice with higher

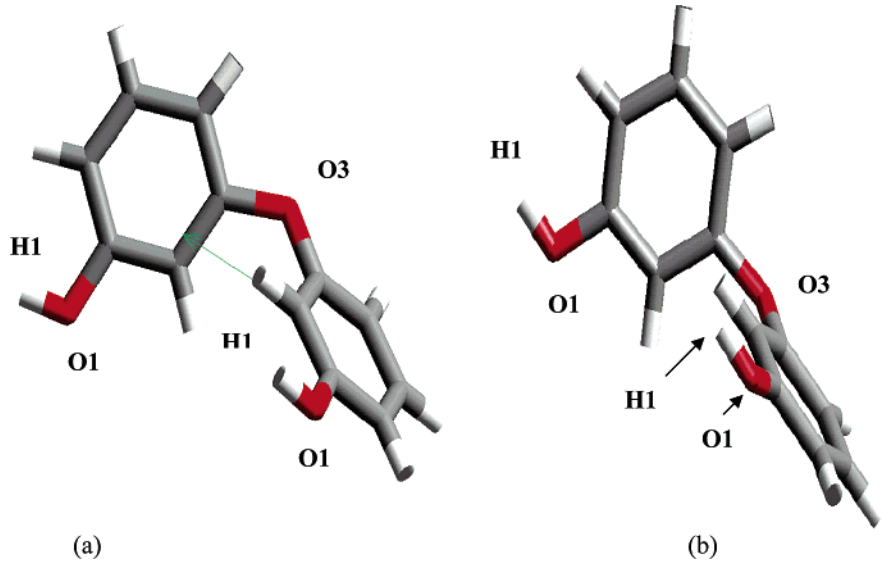

Figure 2. Optimized geometry of the resorcinol dimer in (a) the gas phase and (b) the solvated phase with all the hydrogen and oxygen atoms of the molecule labeled.

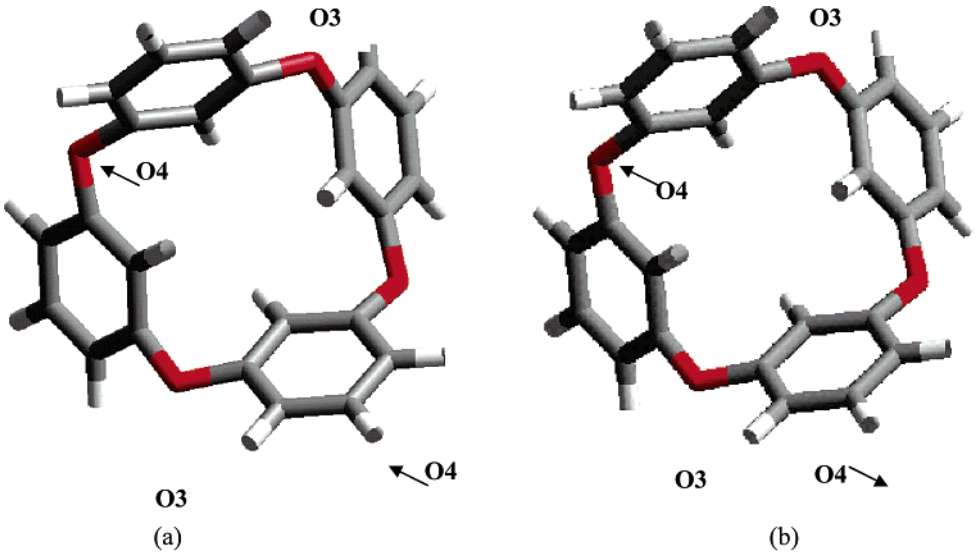

Figure 3. Optimized geometry of the resorcinol tetramer in (a) the gas phase and (b) the solvated phase with all the hydrogen and oxygen atoms of the molecule labeled.

TABLE 1: Global and Local Reactivity Index Parameters for the Resorcinol Monomer (in the Gas Phase) and in the Solvated State

mol	GS	atom	s_x^+	s_x^-	s_x^-/s_x^+	s_x^+/s_x^-
Res1	1.23	O1	0.159	0.212	0.751	1.333
		H1	0.164	0.251	0.653	1.530
		O2	0.162	0.215	0.753	1.327
		H2	0.164	0.253	0.648	1.542
Res1s	1.37	O1	0.152	0.193	0.787	1.269
		H1	0.153	0.213	0.718	1.387
		O2	0.156	0.198	0.787	1.265
		H2	0.161	0.225	0.715	1.392

TABLE 2: Global and Local Reactivity Index Parameters for the Resorcinol Dimer (in the Gas Phase) and in the Solvated State

mol	GS	atom	s_x^+	s_x^-	s_x^-/s_x^+	s_x^+/s_x^-
Res2	2.32	O1	0.134	0.197	0.680	1.470
		H1	0.127	0.213	0.596	1.677
		O3	0.012	0.008	1.500	0.071
Res2s	2.41	O1	0.124	0.182	0.681	1.467
		H1	0.118	0.196	0.602	1.661
		O3	0.013	0.008	1.625	0.615

TABLE 3: Global and Local Reactivity Index Parameters for the Resorcinol Tetramer (in the Gas Phase) and in the Solvated State

mol	GS	atom	s_x^+	s_x^-	s_x^-/s_x^+	s_x^+/s_x^-
Res4	2.68	O3	0.065	0.049	1.326	0.661
		O4	0.059	0.042	1.404	0.711
Res4s	2.98	O3	0.057	0.043	1.325	0.754
		O4	0.048	0.037	1.297	0.770

nucleophilicity. The monomers of resorcinol therefore can combine in the presence of water. As the monomers combine to form dimers or higher oligomers, their activity toward interaction with the clay interlayer increases. Localized reactivity calculation thus can propose the path of the interaction and its feasibility. Considering the real situation, which involves all the constituents of the process such as the clay matrixes, the interlayer cation, and the water molecule at its first hydration layer, dimer will be the potential candidate to start with. We will as well look at the situation with tetramer later in this study.

Known Features of Clay Swelling. Experimentally it is known that the *d* spacing is related to the number of water layers surrounding the exchangeable cation. Depending on the extent

TABLE 4: Global and Local Reactivity Index Parameters for the Resorcinol Monomer (in the Gas Phase) and in the Hydrated State (While Interacting with a Single Water Molecule)

mol	GS	atom	s_x^+	s_x^-	s_x^-/s_x^+	s_x^+/s_x^-
Res1	1.23	O1	0.159	0.212	0.751	1.333
		H1	0.164	0.251	0.653	1.530
		O2	0.162	0.215	0.753	1.327
		H2	0.164	0.253	0.648	1.542
Res1s	1.37	O1	0.167	0.235	0.710	1.407
		H1	0.152	0.238	0.638	1.565
		O2	0.168	0.234	0.717	1.392
		H2	0.156	0.245	0.636	1.562

of increment in basal spacing between two smectite sheets, two types of swelling mechanism are proposed:[54] (1) crystalline swelling and (2) osmotic swelling. Crystalline swelling occurs for a situation with a monolayer of water adsorption around the cation, held by hydrogen bonding to the hexagonal network of oxygen atoms. This could result an increase of *d* spacing in the range of about 10−20 Å. The osmotic swelling is the

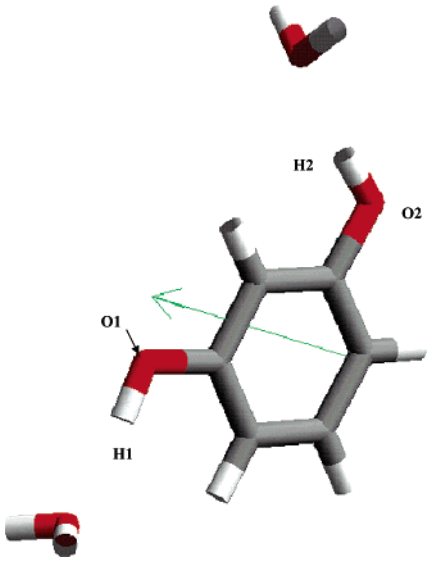

Figure 4. Optimized geometry of the resorcinol monomer in the hydrated phase with two water molecules approaching the hydroxyl sites with all the hydrogen and oxygen atoms of the molecule labeled.

phenomenon when the interlayer spacing increases abruptly to 30−40 Å with higher water content due to the interaction of the layer, which is beyond the scope of this study.

As mentioned earlier, we have used the model of the montmorillonite type clays with structural formula $MSi_8Al_3MgO_{20}(OH)_4$ and optimized the structure in their unhydrated form using periodic ab initio calculations.[24] The internal coordinate matches with the available experimental values. The deviation is mostly at the basal oxygen atoms of the tetrahedral sheet, which is due to the rotation of SiO_4 tetrahedra by 13.2° and a tilt of 4.6° on average. This is in close agreement with the numbers generated by Bridgeman et al.[55] with a rotation of 18.4° and a tilt of 6.5°. It is observed that for montmorillonite the hydroxyl hydrogen attached to the octahedral aluminum makes an angle of 24.12° with the $a-b$ plane, which is in close conformity with the observation of Giese et al.[56] By minimizing the electrostatic energy of pyrophyllite, they predicted the angle to be 26° with respect to the hydroxyl hydrogen.

Structural Changes in the Clay Interlayer before and after Hydration Both in the Presence and Absence of Resorcinol Oligomer. We have established that[24] the location of the cation is dependent on the source of layer charge originating from the octahedral/tetrahedral substitution for the specific clay structure. When the layer charge originates from the substitution of octahedral aluminum, the hydroxyl hydrogen shows an inclination to stabilize the cation and the cation stay on top of it with a larger distance from the center of the layer charge. On the other hand, for the tetrahedral substitution at the tetrahedral silicon, the cation interacts more favorably with surface hydroxyl. The distance between cation and surface hydroxyl is less, compared to the octahedral case, and thus causes a restricted swelling phenomenon.

We first optimized the unhydrated montmorillonite structure followed by optimization of the hydrated structure, with sodium as the exchangeable cation and 5 water molecules surrounding the cation. To visualize the effect of water on the swelling phenomenon in the presence of the resorcinol oligomer, we have concentrated only on the first shell of hydration. In the swelling process, each cation is first hydrated to its first hydration shell; the further increment in the hydration layer is dependent on the amount of humidity. However, the increase in humidity does not favorably increase the layers around the cation. The water then may reside as a nonbonded molecule in the bulk and does not contribute much toward the swelling phenomenon. The first layer therefore will be the best choice to explore the electronic trend involving the cation and the clay interface. The first hydration shell also can be the domain to look at the interwater H-bonding process, which may be pronounced or suppressed depending on the location of the cation over the clay surface.

For the optimization of the montmorillonite structure in the unhydrated form with sodium as the monovalent exchangeable cation, we relaxed the cation and the top two layers of the tetrahedral silicon and octahedral aluminum/magnesium layer; the bottom two layers were kept fixed throughout the calculation. The results are shown in Table 5.

The hydrated state calculations were performed with the optimum water content around the respective interlayer exchangeable cations according to our previous study[24] where the forced boundary condition was applied. The number of water molecules around monovalent cations is 5 and that for bivalent cations is 3 in the first hydration shell. In terms of the first hydration layer, the result matches with our earlier grand canonical Monte Carlo (GCMC) simulation[20] and also with the experiment. It is observed that a bivalent metal like calcium gets sandwiched between two layers of water molecules consisting of three water molecules each. Our calculation successfully reproduces the top layer of water, which is acting as the first hydration shell.

TABLE 5: Cell Parameters for Bulk Clay and Systems with Intercalated Resorcinol Oligomers Both with and without Solvation

complex	a (Å)	b (Å)	c (Å)	α (deg)	β (deg)	γ (deg)
clay[a]	5.167	8.890	14.692	89.84	97.85	89.91
clay[b]	5.197	8.994	14.881	90.16	97.11	90.65
C+R2[a,c]	5.162	8.886	14.687	89.99	99.50	89.96
C+R2[b,c]	5.176	8.898	14.113	90.08	97.98	90.08
C+R4[a,c]	5.131	8.950	14.688	90.02	99.40	89.93
C+R4[b,c]	5.166	8.973	14.234	90.39	97.57	90.01

[a] Stands for calculation with no water. [b] Stands for calculation with water. [c] C stands for clay. R2 stands for the dimer of resorcinol, and R4 stands for the tetramer of resorcinol.

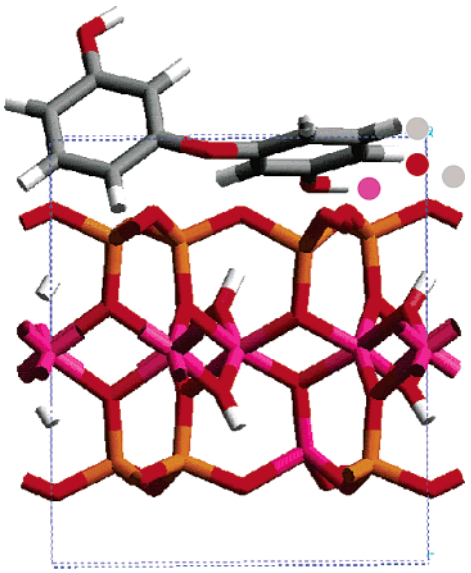

Figure 5. Optimized geometry of the resorcinol dimer over the montmorillonite clay structure with exchangeable cation and water molecules.

The cell parameters for the hydrated system are also shown in Table 5. We have seen from the results that the montmorillonite clay interlayer swells to 14.881 Å, which is close to the experimental observation[18] (15.1 Å). Both the calculations in the hydrated and unhydrated form were performed in the presence of sodium as the interlayer cation. After optimizing the unhydrated and hydrated clay cells of the montmorillonite, we calculated those structures in the presence of resorcinol dimer and tetramer. A model of the calculation with one water molecule for visual clarity is shown in Figure 5. We have placed the resorcinol molecule parallel to the surface with the hydroxyl pointed toward the exchangeable cation surrounded by water molecules. The results are shown in Table 5. In the presence of the resorcinol tetramer, there is an elongation in the a direction and a negligible quenching in the c direction for all the resorcinol oligomers in the unhydrated clay situations. However, there is an observable change in the cell parameters when the calculations are performed in the hydrated phase. A quenching in the c direction was observed for all the cases in the presence of the resorcinol oligomer. The quenching decreases with increase in the size of the resorcinol oligomer from dimer to tetramer and indicates the resorcinol oligomer uses the water for intermolecular bonding. Accordingly, there is not enough water to pursue the swelling phenomenon. Thus the periodic calculation

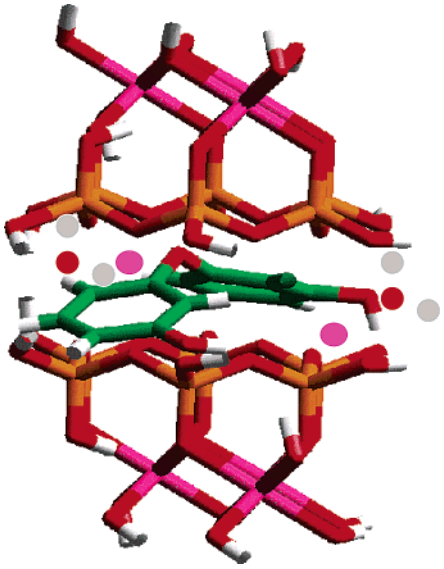

Figure 6. The model to show the fitting of the resorcinol dimer within the interlayer space of clay montmorillonite in the presence of exchangeable cation sodium and water molecules.

TABLE 6: Interaction Energy for Resorcinol Oligomers Intercalated in Clay in the Presence of Water

	energy (kJ/mol)		
complex	clay resorcinol complex	clay + resorcinol	IE (kJ/mol)
CR2W[a]	−17131.2	−17122.05	−9.15
CR4W[b]	−23421.4	−23418.85	−3.55

[a] Represents clay with resorcinol dimer in the presence of water. [b] Represents clay with resorcinol tetramer in the presence of water.

validates the prediction of the reactivity index calculation. The water here is helping the resorcinol oligomer to stabilize through an intermolecular H-bonding network. Now we need to test the respective stability of the individual oligomer (dimer and tetramer) inside the clay interlayer to compare the fitting of the resorcinol oligomers inside the clay structure.

The interaction energy for the resorcinol oligomers with the clay structures is calculated using the following expression:

$$\text{TE(clay/resorcinol complex)} - \text{TE[clay + resorcinol]} = \text{interaction energy}$$

where TE = total energy. A model including the resorcinol tetramer in the presence of water, exchangeable cation, and the clay structure is shown in Figure 6. The results of the interaction energy calculation are shown in Table 6. This interaction energy is calculated to rationalize our earlier observation from reactivity index results of the independent molecule and the periodic calculation to see the molecular fitting of the resorcinol dimer or tetramer in the interlayer of the montmorillonite clay. We have calculated the interaction energy for two sets of resorcinol molecules to compare the probable pathway of the growth of the resorcinol oligomers inside the interlayer of the montmorillonite clay. The result shows that the resorcinol dimer is more stable by ~6 kJ/mol than the tetramer inside the clay interface. The dimer can favorably interact with other resorcinol dimers present in the interlayer through H-bonding and as well interact with the clay structure without solvation. This matches our prediction from the reactivity index. The lower stability of the tetramer can be explained from its lower nucleophilicity which will not favorably interact with the clay interlayer.

Here, we are trying to figure out the nature of the resorcinol conformation in the interlayer. We have seen that the material synthesized is soft; this prescribes that the interlayer resorcinol variety will probably not be the tetramer, otherwise the synthesized film would be much harder. Hence, the dimer will be the favorable piece to bind with other dimers through H-bonding and through hydration with the water present in the interlayer. At the same time, we can say from the interaction energy that whatever the size of the resorcinol oligomer it is stable inside the clay moiety and from the periodic calculation study as well we can say that any of the oligomers like dimer or tetramer can exist in the interlayer space comfortably. Considering all aspects, including growth of the oligomer inside the interlayer of the clay nanocomposite based on the periodic study and the reactivity index study and also from the solvation and hydration account, the most favorable size of the oligomer is dimer.

Conclusion

This is the first study to propose the structural features of the resorcinol−clay nanocomposite, where resorcinol is incorporated in the clay interlayer. The experimental study revealed that resorcinol in the interlayer is stable even above the boiling temperature, which proposed that resorcinol molecules might be oligomerizing. We have used both periodic ab initio and localized reactivity index calculations to propose the mechanism of synthesis to monitor the dominating process in the resorcinol oligomerization in terms of its interaction with the clay interlayer in the presence and absence of water. By comparing both solvation and hydration, the plausible configuration of the resorcinol oligomer inside the clay interlayer has also been predicted. The resorcinol molecule is competing with the exchangeable cation when existing as a monomer, and then with the help of water it undergoes hydration. This hydration favors the oligomerization of the resorcinol monomer. Our localized reactivity index calculation categorically has shown that for the resorcinol molecule the hydration is the primary process and is never solvated. It is observed that the relative nucleophilicity−electrophilicity trend is the same until the dimer, where the nucleophilicity increases after solvation and electrophilicity decreases, while the trend is reversed for the tetramer case. Through the periodic calculations, we have shown that the initial hydration is consuming water before the oligomers are formed. Once the oligomers are formed, they combine with each other inside the interlayer through H-bonding and hence there is a considerable quenching. The quenching is less pronounced when the resorcinol tetramer is incorporated. The interaction energy results show that the tetramer is less stable in comparison to the dimer, which can be explained in terms of reactivity index results. At this point we can obviously say that the resorcinol combines through the monomer and the dimer is the most stable inside the clay interlayer. The little quenching after the incorporation of the resorcinol oligomer is due to the intermolecular H-bonding. We still need to look at the situation with higher humidity and other possible combination factors related to the resorcinol molecule, which is the topic of our future study.

Acknowledgment. A part of this study was financially supported by the Budget for Nuclear Research of the Ministry of Education, Culture, Sports, Science and Technology, based on the screening and counseling by the Atomic Energy Commission.

References and Notes

(1) Theng, B. K. G. In *Formation and Properties of Clay−Polymer Complexes*; Elsevier: New York, 1979; p 137.

(2) Kato, C.; Kuroda, K.; Misawa, M. *Clays Clay Miner.* **1979**, *27*, 129.
(3) Mehrotra, V.; Giannelis, E. P. *Solid State Ionics* **1992**, *51*, 115.
(4) Giannelis, E. P. *Chem. Mater.* **1990**, *2*, 627.
(5) Messerssmith, P. B.; Giannelis, E. P. *Chem. Mater.* **1993**, *5*, 1064.
(6) Blumstein, A. *J. Polym. Sci.* **1965**, *A3*, 2653.
(7) Friendlander, H. Z.; Frick, C. R. *J. Polym. Sci.* **1964**, *B2*, 475.
(8) Solomon, D. H. *J. Appl. Polym. Sci.* **1968**, *12*, 1253.
(9) Glaveti, O. L.; Polak, L. S. *Neftekhim* **1963**, *3*, 905.
(10) Lan, T.; Kaviratna, P. D.; Pinnavaia, T. J. *Chem. Mater.* **1994**, *6*, 573.
(11) Alexandre, M.; Dubois, P. *Mater. Sci. Eng.* **2000**, *28*, 1.
(12) Usuki, A.; Kojima, Y.; Kawasumi, M.; Okada, A.; Fukushima, Y.; Kurauchi, T.; Kamigaito, O. *J. Mater. Res.* **1993**, *8*, 1179.
(13) Yano, K.; Usuki, A.; Okada, A.; Kuraychi, T.; Kamigaito, O. *Polym. Prepr.* (*Am. Chem. Soc. Polym. Div.*) **1991**, *32*, 65.
(14) Yano, K.; Usuki, A.; Okada, A.; Kuraychi, T.; Kamigaito, O. *J. Polym. Sci.*: *Polym. Chem.* **1993**, *31*, 2493.
(15) Gardebien, F.; Goudel-Siri, A.; Bredes, J. L; Lazzarouni, R. *J. Phys. Chem. B* **2004**, *108*, 10678−10686.
(16) Wang, Z. M.; Chung, T. C.; Gilman, J. W.; Manias, E. *J. Polym. Sci. B*: *Polym. Phys.* **2003**, *41*, 3173.
(17) Kuppa, V.; Menakanit, S.; Krishnamoorti, R.; Manias, E. *J. Polym. Sci. B*: *Polym. Phys.* **2003**, *41*, 3285.
(18) Ebina, T.; Mizukami, F. Japanese Patent application 2003-315780 and 2003-338378, 2003.
(19) Ebina, T.; Iwasaki, T.; Chatterjee, A.; Katagiri, M.; Stucky, G. D. *J. Phys. Chem. B* **1997**, *101*, 1125.
(20) Chatterjee, A.; Iwasaki, T.; Ebina, T.; Hayashi, H. *Appl. Surf. Sci.* **1997**, *121/122*, 167.
(21) Chatterjee, A.; Iwasaki, T.; Hayashi, H.; Ebina, T.; Torri, K. *J. Mol. Catal. A* **1998**, *136*, 195.
(22) Chatterjee, A.; Iwasaki, T.; Ebina, T.; Miyamoto, A. *Comput. Mater. Sci.* **1999**, *14*, 119.
(23) Chatterjee, A.; Iwasaki, T.; Ebina, T. *J. Phys. Chem. A* **2000**, *104*, 8216.
(24) Chatterjee, A.; Ebina, T.; Onodera, Y.; Mizukami, F. *J. Chem. Phys.* **2004**, *120*, 3414.
(25) Pearson, R. G. *J. Am. Chem. Soc.* **1983**, *105*, 7512.
(26) Pearson, R. G. *J. Chem. Educ.* **1987**, *64*, 561.
(27) Parr, R. G.; Yang, W. *J. Am. Chem. Soc.* **1984**, *106*, 4049.
(28) Geerlings, P.; De Proft, F.; Langenaekar, W. *Chem. Rev.* **2003**, *103*, 1793 and references therein.
(29) Nguyen, L. T.; Le, T. N.; De Proft, F.; Chandra, A. K.; Langenaeker, W.; Nguyen, M. T.; Geerlings, P. *J. Am. Chem. Soc.* **1999**, *121*, 5992.
(30) Langenaeker, W.; De Proft, F.; Geerlings, P. *J. Phys. Chem. A* **1998**, *102*, 5944.
(31) Chandra, A. K.; Geerlings, P.; Nguyen, M. T. *J. Org. Chem.* **1997**, *62*, 6419.
(32) Sivanesan, D.; Amutha, R.; Subramanian, V.; Nair, B. U.; Ramaswami, T. *Chem. Phys. Lett.* **1999**, *308*, 223.
(33) Pearson, R. G.; Parr, R. G. *J. Am. Chem. Soc.* **1983**, *105*, 7512.
(34) Yang, W.; Mortier, M. J. *J. Am. Chem. Soc.* **1986**, *108*, 5708.
(35) Teter, M. P.; Payne, M. C.; Allen, D. C. *Phys. Rev. B* **1989**, *40*, 12255.
(36) Payne, M. C.; Teter, M. P.; Allan, D. C.; Arias, T. A.; Johannopoulos, J. D. *Rev. Mod. Phys.* **1992**, *64*, 1045.
(37) Perdew, J.; Zunger, A. *Phys. Rev. B* **1981**, *23*, 5048.
(38) Winkler, B.; Milman, V.; Payne, M. C. *Am. Mineral.* **1994**, *79*, 200.
(39) Perdew, J. P. *Phys. Rev. B* **1986**, *33*, 8822.
(40) Becke, A. D. *Phys. Rev. A* **1988**, *33*, 3098.
(41) Laasonen, K.; Csajka, M.; Parrinello, F. M. *Chem. Phys. Lett.* **1992**, *194*, 172.
(42) Lee, C.; Vanderbilt, D.; Laasonen, K.; Car, R.; Parrinello, M. *Phys. Rev. B* **1993**, *47*, 4863.
(43) Garcia, A.; Elsasser, C.; Zhu, J.; Louie, S. G.; Cohen, M. L. *Phys. Rev. B* **1992**, *46*, 9829.
(44) Monkhorst, H. J.; Pack, J. D. *Phys. Rev. B* **1976**, *13*, 5188.
(45) Kohn, W.; Sham, L. J. *Phys. Rev. A* **1965**, *140*, 1133.
(46) Becke, A. *J. Chem. Phys.* **1988**, *88*, 2547.
(47) Lee, C.; Yang, W.; Parr, R. G. *Phys. Rev. B* **1988**, *37*, 786.
(48) Bock, C. W.; Trachtman, M. J. *Phys. Chem.* **1994**, *98*, 95.
(49) Boys, S. F.; Bernardi, F. *Mol. Phys.* **1970**, *19*, 553.
(50) Newman, A. C. D.; Brown, G. In *Chemistry of Clays and Clay Minerals*; Newman, A. C. D., Ed.; Minerological Society Monograph No. 5; Minerological Society: London, 1974; p 10.
(51) Roy, R. K.; Krishnamurthy, S.; Geerlings, P.; Pal, S. *J. Phys. Chem. A* **1998**, *102*, 3746.
(52) Chatterjee, A.; Iwasaki, T.; Ebina, T. *J. Phys. Chem. A* **2001**, *105*, 10694.
(53) Chatterjee, A.; Ebina, T.; Iwasaki, T.; Mizukami, F. *J. Chem. Phys.* **2003**, *118*, 10212.
(54) Luckham, P. F.; Rossi, S. *Adv. Colloid Interface Sci.* **1999**, *82*, 43.
(55) Bridgeman, C. H.; Buckingham, A. D.; Skipper, N. T.; Pyne, M. C. *Mol. Phys.* **1996**, *89*, 879.
(56) Giese, R. F. *Nature* **1973**, *241*, 15.